Bioelectrochemistry 158 (2024) 108710

Contents lists available at ScienceDirect

Bioelectrochemistry

journal homepage: www.journals.elsevier.com/bioelectrochemistry

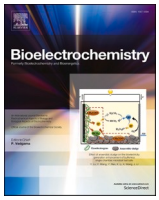

Revealing cellular (poly)sulphide storage in electrochemically active sulphide oxidising bacteria using rotating disc electrodes

Rikke Linssen [a], Sanne de Smit [a], Katharina Röhring (neé Neubert) [b], Falk Harnisch [b], Annemiek ter Heijne [a,*]

[a] Environmental Technology, Wageningen University, P.O. Box 17, Bornse Weilanden 9, 6708 WG, Building Axis z, building nr. 118, 6700 AA Wageningen, the Netherlands

[b] Department of Microbial Biotechnology, Helmholtz-Centre for Environmental Research GmbH – UFZ, Permoserstrasse 15, 04318 Leipzig, Germany

ARTICLE INFO

Keywords:
Biodesulphurisation
Rotating disc electrode
Microbial charge storage
Sulphide oxidising bacteria
Microbial electrochemical technology

ABSTRACT

Sulphide oxidising bacteria (SOB) have the potential to be used for bioelectrochemical removal, i.e. oxidation, of sulphide from waste streams. In anaerobic conditions, SOB are able to spatially separate sulphide removal and terminal electron transfer to an electrode and act as a sulphide shuttle. However, it is not fully understood how SOB anaerobically remove sulphide and store charge equivalents, and where in this process sulphur is formed. Therefore, the redox behaviour of sulphide shuttling SOB was investigated at haloalkaline conditions using a glassy carbon rotating disc electrode (RDE) and cyclic voltammetry. Voltammograms of SOB in the absence and presence of sulphide were compared to voltammograms of abiotic sulphur species solutions. Polysulphide and sulphide showed different redox behaviour, with distinct potentials for oxidation of > -0.3 V (vs. Ag/AgCl) for polysulphide and > -0.1 V for sulphide. Comparing biotic to abiotic experiments lead to the hypothesis that SOB formed polysulphides during anaerobic sulphide removal, which stayed sorbed to the cells. With this study, further steps were taken in elucidating the mechanisms of sulphide shuttling by SOB.

1. Introduction

Haloalkaline sulphide oxidising bacteria (SOB) are chemolithotrophic bacteria that oxidise reduced sulphur compounds such as sulphide (S^{2-}) to elemental sulphur (S^0), thiosulphate ($S_2O_3^{2-}$) and/or sulphate (SO_4^{2-}). In nature, SOB are found in highly saline as well as highly alkaline waters, such as sulphur springs and marine hydrothermal vents [1]. Examples of haloalkaline SOB are *Thioalkalimicrobium, Thioalkalivibrio, Thioalkalispira* and *Alkalilimnicola* [2,3]. The unique ability of SOB to thrive in haloalkaline sulphidic conditions and oxidise reduced sulphur species attract their use in treatment processes to convert toxic and corrosive sulphide to non-hazardous end products like sulphur [4].

One of such treatment processes is the waste gas biodesulphurisation process developed in the 1990 s [5]. In this process, waste gas containing sulphide is exposed to a haloalkaline solution containing SOB in an adsorber column. Thereafter the sulphidic solution is aerated and SOB convert sulphide to sulphur under aerobic conditions. Subsequently, sulphur is removed by decantation or centrifugation, and the liquid stream is again scand to the adsorber column [6]. Recently, it was shown that in the anaerobic absorption column, higher sulphide absorption rates were measured in the presence of SOB compared to abiotic runs [7]. Also, in the anaerobic section of the reactor setup, lower sulphide levels were measured than were expected based on the applied sulphide load and the measured products [8]. It was subsequently confirmed that SOB can remove sulphide in anaerobic conditions and temporarily or spatially separate sulphide removal from terminal electron transfer [9,10], thereby acting as a sulphide shuttle. This means that a storage of charge (equivalents) in SOB needs to take place. It was also discovered that SOB are electroactive and can use electrodes as terminal electron acceptor instead of oxygen [9,11]. Here, SOB were exposed to sulphide under anaerobic conditions, after which SOB removed all sulphide. Subsequently applying anodic potentials ($\geq$-0.1 V vs. Ag/AgCl) resulted in an anodic current, even though no sulphide could be detected in solution. Therefore, it was postulated that SOB store charge or charge equivalents in the form of reduced redox carriers, for instance in cytochromes and quinones, but also sulphur species [10].

Intracellular storage of reduced compounds by microorganisms is

* Corresponding author.
E-mail address: Annemiek.terHeijne@wur.nl (A. ter Heijne).

https://doi.org/10.1016/j.bioelechem.2024.108710
Received 28 June 2023; Received in revised form 11 April 2024; Accepted 12 April 2024
Available online 14 April 2024

common in nature. Bacteria are known to store polysaccharides, polyphosphate, poly-β-hydroxyalkanoates (PHA's), triacylglycerides, and wax esters, among others, in the absence of terminal electron acceptors [12]. However, little is known about the mechanisms of storage of charge equivalents related to sulphide oxidation and subsequent electrochemical activity [13]. Previously we showed that the kinetics of abiotic sulphide oxidation were very similar to the kinetics of electron transfer between SOB and an anode, which could suggest that SOB released sulphide in the presence of an electrode, where the sulphide was subsequently oxidised [11]. If this also caused sulphur deposition on the electrode surface was not experimentally investigated. It has been postulated that anaerobic sulphide removal by SOB is based on storage of polysulphides [10], the product of the equilibrium reaction between sulphide an elemental sulphur (Eq. (1). The chain length, x, of the polysulphides is dependent on, among others, the type of solvent, pH, and temperature.

$$S^{2-} + xS^0 \rightleftharpoons S_{x+1}^{2-} \quad (1)$$

The role of polysulphides in sulphide removal and release of electrons by SOB was not studied. To gain a better understanding of the mechanisms of storage of charge equivalents in SOB during anaerobic sulphide removal, we used a rotating disc electrode (RDE) to investigate the redox behaviour of sulphide shuttling SOB. Cyclic voltammetry (CV) was performed at a glassy carbon (GC) RDE, acting as a stationary or rotating electrode. By comparing voltammograms of sulphide and polysulphide to voltammograms of sulphide shuttling SOB, more insight was gained on the sulphide shuttling mechanisms.

The RDE is conventionally used to investigate electrochemical reactions without living microbial electrocatalysts. To our knowledge only a few publications described the investigation of microorganisms with the use of an RDE. Half of these papers were dealing with microorganisms present on the disc in the form of a biofilm [14–19], the other half worked with planktonic biomass [20–24]. The use of RDE for studying microbial electrochemicals systems is still in need of exploration and validation, and its use for studying sulphur species in combination with microorganisms is entirely untapped. Therefore, in this article we demonstrated the use of the RDE in the investigation of planktonic electroactive bacteria to further develop the use of the RDE in the field of microbiology and related sciences.

2. Materials and methods

2.1. General remarks

A list of used symbols can be found in Table S1. Except when stated otherwise, all chemicals were of at least analytical grade, all solutions were prepared with demineralised water, and all electrode potentials in this work are given versus Ag/AgCl sat. KCl (i.e. 0.2 V vs. standard hydrogen electrode (SHE)). Error margins indicate the standard deviation. The number of independent replicas ranged between 2 and 9, and are listed per sample species in Table S2 and S3. When referring to a mixture of sulphide and polysulphides, this is indicated by the term '(poly)sulphide'. Elemental sulphur can be present in the form of many different allotropes [25], therefore when referring to 'sulphur' or 'elemental sulphur' we generalise all allotropes of non-charged sulphur.

2.2. Biomass harvesting

Reactor effluent containing SOB was harvested from the dual-reactor biodesulphurisation pilot plant stationed at Wageningen University and Research [6] in March 2022, and from a lab scale dual-reactor biodesulphurisation setup in Wetsus, Leeuwarden in October 2022. Harvesting was done aerobically. The effluent was centrifuged for 30 min at 7500 × g (High speed centrifuge Z 36 HK, Hermle LaborTechnik, Germany). To separate SOB from the sulphur, the red-brown SOB layer on top of the pellet was carefully resuspended in 1 M bicarbonate ($NaHCO_3$) buffer (EMSURE Merck, Germany) of pH 8–8.5, keeping most of the white-yellow sulphur layer on the bottom of the pellet intact. The suspension was then washed for at least three times by centrifuging for 10 min at 15000 × g and resuspending the SOB in bicarbonate buffer, until no sulphur layer was visible. After the last washing step, the SOB were aerated overnight by bubbling with compressed air to remove residual sulphur and to fully oxidise the SOB. The SOB content was then measured spectrophotometrically (LCK 138, Hach Lange, USA) and expressed as total nitrogen content [6,9]. The SOB stock, at a biomass content of ~ 200–400 mgN L^{-1}, was then stored at 4 °C.

2.3. Stock solutions

Stock solutions of sulphate (Na_2SO_4, Sigma-Aldrich, USA), sulphide (NaHS, Acros Organics, Belgium) and (poly)sulphide were prepared in batch bottles using water that was made anaerobic by flushing with nitrogen gas. (Poly)sulphide stock was made by dissolving 1 mM sulphide with an excess of chemical grade sulphur powder (Merck, Germany) and incubating overnight at room temperature to reach equilibrium. When (poly)sulphide was taken from the stock with a syringe, care was taken to not suck up the sulphur powder accumulated at the bottom of the bottle. The total sulphide plus polysulphide content was then measured using redox titration with $AgNO_3$ (Titrino Plus, Metrohm, Switzerland). In a mixture of 80 mL 5 wt% NaOH and 10 mL 2.5 wt% NH_3 a 0.1 mL sample was titrated with 0.1 M $AgNO_3$ in triplicate.

2.4. Rotating disc electrode and cyclic voltammetry

The RDE experiments were performed in a 100 mL vessel with a teflon lid (ALS Co., Ltd., Japan) using a potentiostat (Vertex, Ivium Technologies, The Netherlands). The RDE setup (IviumRRDE apparatus, Ivium Technologies, The Netherlands), the working electrode (Rotating ring disc electrode GC Ring/GC Disc Electrode, ALS Co., Ltd., Japan), platinum counter electrode (MW-1033 Coiled platinum counter electrode, Basi, USA), Ag/AgCl (MF-2053 Ag/AgCl (3 M NaCl), reference electrode, Basi, USA) as well as the gas inlet were positioned as shown in Scheme 1. The working electrode, with a disc diameter of 4 mm (12.6

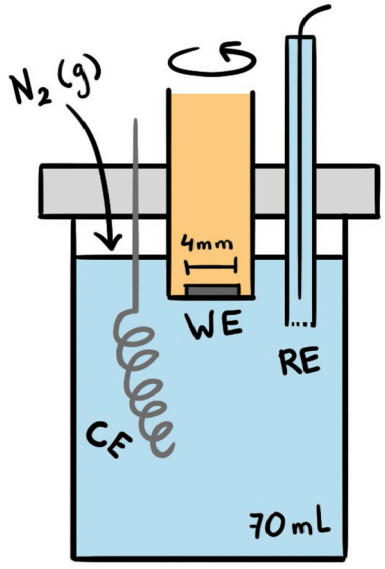

Scheme 1. General setup of the RDE showing the glassy carbon RDE as working electrode (WE), the platinum counter electrode (CE) and the Ag/AgCl reference electrode (RE). The headspace was continuously sparged with nitrogen gas (N_2 (g)) to maintain anaerobic conditions, the total liquid volume was 70 mL. For a photograph of the used setup, see Fig. S1.

mm^2), was polished manually before each experiment using aluminium oxide powder with water on a nylon polishing pad (PK-4 Electrode polishing kit, ProSense, The Netherlands). After polishing, the electrode surface was cleaned in an ultrasonic bath (Branson 5210, Gemini BV, The Netherlands) for 1 min and dried using a nitrogen gas stream. Before each experiment, the 70 mL solution was made anaerobic by flushing with nitrogen or argon gas for at least 15 min. During the experiment, the headspace was flushed with nitrogen or argon gas. All experiments were conducted at room temperature (around 21–25 °C).

All experiments were performed in 1 M bicarbonate ($NaHCO_3$) buffer at pH 8.5, corresponding with the composition of the haloalkaline reactor solution in the biological desulphurisation process [6,26]. Cyclic voltammetry (CV) was performed at 10 mV s^{-1} and rotation rates of 500–6000 rpm. If not mentioned otherwise, the working electrode (WE) potential was cycled between −1.5 and 1.0 V. In this work the scan from −1.5 to + 1.0 V is called the forward scan, the scan from + 1.0 to −1.5 V is denominated the backward scan. The following solutions were tested without SOB: 0.3 and 1 mM sulphide and (poly)sulphide, 0.3 mM sulphide with 0.4–0.8 mM biologically produced sulphur (biosulphur), 100 mM biosulphur, 1 mM sulphite, 1 mM thiosulphate, and 1 mM sulphate. Biosulphur, i.e. sulphur produced by SOB, was used instead of chemically produced sulphur due to its lower hydrophobicity and higher suspendability in water. Biosulphur was harvested from the biodesulphurisation plant at Wageningen University. For an extensive overview of all tested conditions, see Table S2 and Table S3.

Electrochemical analysis in the presence of SOB was performed on aerated or sulphidic SOB. Aerated SOB were previously thoroughly aerated so all residual sulphur species were oxidised. Sulphidic SOB were prepared by incubating aerated SOB with 0.2–0.3 mM sulphide for 15 min in anaerobic conditions. During this incubation period, SOB (partly) removed sulphide from solution. A sample was taken before starting the CV to measure the sulphide content of the solution. Experiments were performed with 15 or 60 mgN L^{-1} aerobic and sulphidic SOB at 1000, 3000, 5000 or 6000 rpm, and at 10 or 25 mV s^{-1}.

2.4.1. Processing of voltammograms and electrochemical data analysis

All CV data was processed in Microsoft Excel. For studying SOB at different conditions, data was pooled over various runs (up to 9 runs in total) to even out variations in biomass concentrations, rotation speed, scan rate, etc.

Commonly, the first cycle of CV is not analysed as the signal is 'disturbed' by chemically irreversible reactions and several cycles are performed to establish a steady-state. However, the investigated redox processes of sulphur species are not chemically reversible. Some products are lost in the form of inert sulphate (that cannot be reduced electrochemically) or elemental sulphur that may cause electrode surface blockage. Therefore, in this study, the first cycle of CV was used for analysis, unless specified otherwise.

Using the Nernst equation the redox potential of a half reaction E_{eq} was calculated (Eq. (2)) (S.1).

$$E_{eq} = E^0 - \frac{RT}{nF}\ln K - 0.2V \tag{2}$$

Here n is the number of electrons transferred per mol reaction and F is the Faraday constant (96485C mol^{-1}), where R is the universal gas constant (8.13 J K^{-1} mol^{-1}), T is the temperature in Kelvin and K is the reaction quotient (as calculated using Equation S2 in the supplementary information). The redox potential is converted from tabulated values vs. SHE to Ag/AgCl by subtracting 0.2 V.

When applicable, for CVs at a stationary electrode the formal potential E_f was determined from the arithmetic mean of anodic peak potential $E_{P.A}$ and cathodic peak potential $E_{P.C}$ (Eq. (3)).

$$E_f = \frac{E_{P.A} - E_{P.C}}{2} \tag{3}$$

For CVs at a rotating electrode, the inflection point E_i of the voltammogram were determined using the first derivative of the voltammogram (DCV). Before calculating the DCV, the voltammogram was smoothed using moving average at an interval of 30 mV.

2.4.2. Product selectivity

As each cycle only a small amount of reactant was oxidised (in the order of μM) it was not possible to measure the products formed per cycle. Therefore product selectivity for sulphur formation was determined using CV data. The voltammogram of buffer and aerated SOB provided the (pseudo)capacitive background current between −1.5 and + 1.0 V. Therefore it can be assumed for all other voltammograms that anodic and cathodic current in this potential range, other than this background signal, originated from oxidation of (poly)sulphide and reduction of its products. It can be assumed that (poly)sulphide is oxidised to sulphur, sulphite, thiosulphate, or sulphate, all which could not be reduced at the applied conditions (3.1.1). Therefore, it could be assumed all reductive current originated from sulphur deposited at the electrode surface. By taking the scan rate into account, the current was integrated with time for anodic and cathodic current (Eq. (5)), and the total charge produced during (poly)sulphide oxidation (in the forward scan) and supplied during sulphur reduction (in the backward scan) was determined (for an example calculation see S.2). Assuming oxidation of (poly)sulphide and reduction of sulphur both involve the transfer of two electrons, the selectivity of (poly)sulphide oxidation towards sulphur could be calculated (Eq. (6)).

$$Q = \int_{t.start}^{t.end} I \bullet dt \tag{5}$$

$$S_{S^0} = \frac{Q_{red}}{Q_{ox}} \bullet 100\% \tag{6}$$

Here Q is total charge harvested from reduction (*red*) and oxidation (*ox*) charge in C, t the time in s, I the current in A, S_{S^0} the product selectivity for sulphur in %. An example calculation can be found in S.2.

2.5. Chemical analysis

Liquid samples were filtered using a 0.2 μm filter (Chromafil Xtra PES, Macherey-Nagel, Germany) to remove solids such as biomass. Directly after filtration, the sulphide content of the bulk solution was spectrophotometrically measured (LCK 653 m Hach-Lange, country) at a 2–8 × dilution with 0.1 M ZnAcetate [10].

X-ray fluorescence (XRF) was used to analyse sulphur precipitation at the RDE surface. The RDE surface was measured after thorough polishing and after CV scan between −0.3 to 1.0 V and back to 0.0 V of 0.3 mM (poly)sulphide at 3000 and 6000 rpm. The surface was gently rinsed with water and dried with nitrogen gas before measurement. The electrode was put face down in the sampling cup. Samples were analyzed using a wavelength-dispersive X-ray fluorescence (WDXRF) spectrometer S6 Jaguar (Bruker AXS), equipped with Rh X-ray tube, set of analyzer crystals (LiF (200), PET, and XS-55), flow counter for light element detection, and scintillation counter for heavy elements. All measurements were carried out using a standard method with reduced helium flow applied for about 20 min per sample. Samples were quantified using the SMART-QUANT standardless quantification method (Bruker AXS).

3. Results and discussion

3.1. Electrochemical behaviour of (poly)sulphide at glassy carbon electrodes in haloalkaline solution

To better understand the electrochemical behaviour of sulphide shuttling SOB, we first needed to characterise the electrochemical

behaviour of sulphide and polysulphide, and their oxidation products. In general, it can be assumed that when sulphide (depending on pH in the form of hydrogen sulphide (H_2S), bisulphide (HS^-), or sulphide (S^{2-})) is oxidised electrochemically, it is converted to sulphur (Eq. (7)) and/or sulphate (Eq. (8)) [27]. In the anaerobic conditions applied, other possible products of sulphide oxidation are sulphite (Eq. (9)) and thiosulphate (Eq. (10)).

$$HS^- \rightarrow S^0 + 2e^- + H^+ \quad (7)$$

$$HS^- + 4H_2O \rightarrow SO_4^{2-} + 8e^- + 9H^+ \quad (8)$$

$$HS^- + 3H_2O \rightarrow SO_3^{2-} + 6e^- + 7H^+ \quad (9)$$

$$2HS^- + 8H_2O \rightarrow S_2O_3^{2-} + 8e^- + 9H^+ \quad (10)$$

To examine the redox behaviour of different sulphur species, we performed CV on solutions containing 1 mM sulphide, (poly)sulphide, sulphur, thiosulphate, sulphite, and sulphate. The expected sulphur redox reactions, their corresponding redox potentials E_{eq}, the measured peak potentials and the formal potentials E_f are shown in Table 1.

3.1.1. Sulphur, thiosulphate, sulphite, and sulphate

To understand the redox behaviour of possible sulphide oxidation products we performed CV on sulphur, thiosulphate, sulphite and sulphate. In anaerobic conditions, 10 mV s^{-1}, and 0 rpm, the voltammogram of the bicarbonate buffer showed a slight background signal of several μA. When rotation was applied, a current plateau appeared for potentials below −0.5 V if oxygen was present (Fig. S8). The voltammograms of 1 mM sulphate did not differ from the background solution (bicarbonate buffer), neither at 0 or 3000 rpm. The absence of peaks for sulphate was expected, since sulphate is electrochemically inert at the used conditions [28]. Voltammograms of suspended sulphur at 3000 rpm did not differ from the background, except for a small increase in current of 5 to 10 μA at 1.0 V which could indicate the presence of trace amounts of thiosulphate (Fig. 1B). This showed that sulphur present in suspension [29] did not interact with the electrode.

The voltammogram of 1 mM thiosulphate showed an anodic peak $E_{P.ATs}$ centred at 0.95 V with a peak current of 39 μA (Fig. 1A, Table 1). Thiosulphate did not show a cathodic peak in the potential as low as −1.5 V, at both a rotating and a stationary electrode. At a glassy carbon electrode at pH 5 thiosulphate is known to oxidise to tetrathionate at potentials higher than 1 V [30]. In the applied conditions, thermodynamic calculations indicate that oxidation of thiosulphate to tetrathionate is possible at potentials higher than −0.18 V. Therefore peak $E_{P.ATs}$ can be assigned to oxidation of thiosulphate to tetrathionate. The voltammogram of sulphite showed an anodic peak $E_{P.ASt}$ centred at 0.67 V with a peak current of 14 μA (Fig. 1A, Table 1), and an absence of cathodic current peaks. Theoretically, sulphite can only be further oxidised to sulphate and the oxidation of sulphite to sulphate is possible from an E_{eq} more positive than −0.89 V. At pH 8 and a glassy carbon electrode, Ojani et al (2002) observed an oxidation peak centred at 0.65 V [31]. Therefore, we assigned $E_{P.ASt}$ to the oxidation of sulphite to sulphate.

3.1.2. Sulphide

At a stationary electrode, CVs of solutions containing 1 mM sulphide (Fig. 2A) showed one broad anodic peak $E_{P.AS}$ centred at 0.26 V, starting at −0.1 V and reaching a peak current of 10 μA. Additionally, one cathodic peak $E_{P.CS}$ was observed centred at −0.84 V, also reaching peak current of 10 μA, leading to a midpoint potential of −0.29 V. Oxidation of sulphide is known to produce sulphur, thiosulphate, sulphite, and sulphate, but as no sulphite or thiosulphate oxidation peaks were observed sulphide was either oxidised to sulphur or sulphate. Based on thermodynamic calculations (SI section S.1) the equilibrium potential E_{eq} for oxidation of sulphide to sulphur is −0.45 V and for further oxidation of sulphur to sulphate is −0.59 V, therefore $E_{P.AS}$ could be assigned to oxidation of sulphide to both sulphur and sulphate. Sulphate is electrochemically inert at the used conditions, therefore we assign cathodic peak $E_{P.CS}$ only to the reduction of sulphur to sulphide. Of the current harvested during oxidation, 39 ± 7 % was recovered in the cathodic wave, which confirmed that part of sulphide is oxidised to either chemically inert sulphur or sulphate.

Redox behaviour of sulphide at different rotation speeds

While for 1 mM sulphide increasing the rotation speed of the electrode from 0 to 500 resulted in a doubling of the anodic current at $E_{P.AS}$ and a five times increase of cathodic peak current at $E_{P.CS}$, a further increase to 5000 rpm did not result in a much higher current output (Fig. 2B). By rotating faster, the convective flow of solution towards the electrode surface increased, which resulted in a decrease of thickness of the stagnant diffusion layer. The thinner the stagnant diffusion layer, the faster solutes could diffuse towards the electrode. After 500 rpm the current did not increase, which indicated that at ≥ 500 rpm sulphide oxidation was not limited by transfer of mass at any studied potential, and was therefore limited by the rate of electron transfer to the electrode. The potential and shape of cathodic peak $E_{P.CS}$ at different rotation speeds differed slightly between scans. These differences in peak shape are most likely attributed to differences in sulphur allotropes formed.

Similar to CVs without rotation, during CV of 1 mM sulphide at the different rotation speeds of 500 to 5000 rpm (Fig. 2B-C), a cathodic peak

Table 1
Sulphur redox reactions assumed to take place in this study. The redox reactions are written as oxidation reactions. Tabulated values show the calculated redox potential (E_{eq}), measured anodic peak potential ($E_{P.A}$) and current ($I_{P.A}$), measured cathodic peak potential ($E_{P.C}$) and current ($I_{P.C}$), calculated formal potential (E_f), and selectivity (S_{S^0}). Experimental values are taken from voltammograms obtained at 1 mM reactant concentration, 0 rpm and 10 mV s^{-1}. Potentials are given in V vs. Ag/AgCl.

	Reaction name	Reaction equation (redox reaction written as oxidation reactions)	E_{eq}(V)[a]	$E_{P.A}$(V)	$I_{P.A}$(μA)	$E_{P.C}$(V)	$I_{P.C}$(μA)	E_f(V)[d]	S_{S^0}(%)
R1	Sulphide oxidation, to elemental sulphur	$HS^- \rightarrow S^0 + 2e^- + H^+$	−0.45	0.26	10	-0.84	-8	-0.29	39 ± 7
R2	Sulphur oxidation to sulphate	$S^0 + 4H_2O \rightarrow SO_4^{2-} + 6e^- + 8H^+$	−0.59						
R3	Polysulphide oxidation to elemental sulphur [b]	$S_X^{2-} \rightarrow S^0 + 2e^-$	- 0.47	-0.10	6	-0.92	-27	-0.41	94 ± 5
R4	Polysulphide catenation [c]	$S_X^{2-} + S_Y^{2-} \rightarrow S_{X+Y}^{2-} + 2e^-$							
R5	Sulphite oxidation to sulphate	$SO_3{}^2 + H_2O \rightarrow SO_4^{2-} + 2e^- + 2H^+$	−0.89	0.67	14				
R6	Thiosulphate oxidation to tetrathionate	$2S_2O_3{}^2 \rightarrow S_4O_6^{2-} + 2e^-$	−0.18	0.95	39				

[a] Redox potentials of redox couples are calculated based on 1 mM reactant and a sulphate concentration of 0.01 mM, pH 8.5 and 30 °C (SI section S.1).
[b] Assuming average chain length of X = 5.
[c] Depending on the pH, polysulphides exists with different chain lengths, here denoted by X and Y.
[d] Formal potential is calculated according to Eq. (3).

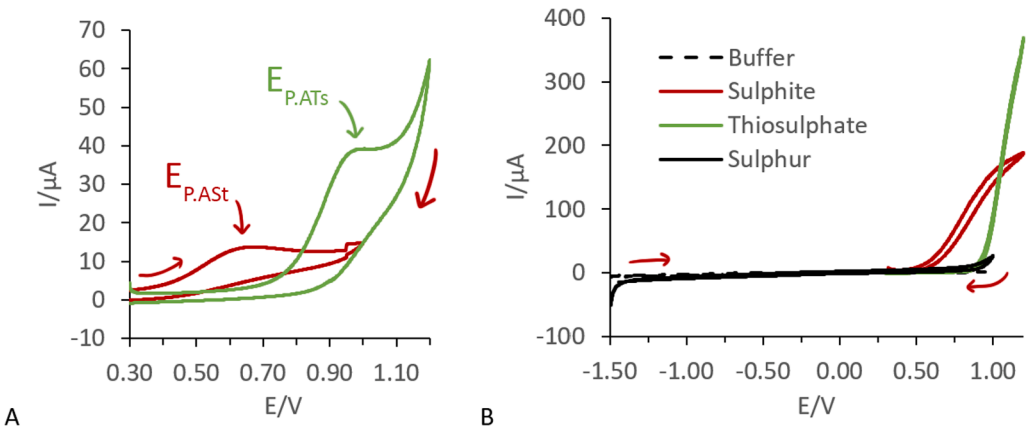

Fig. 1. A) Cyclic voltammograms of 1 mM sulphite (St) and thiosulphate (Ts) at 0 rpm. Indicated are anodic peak potentials $E_{P.A}$. B) cyclic voltammograms of buffer, 1 mM sulphite, 1 mM thiosulphate, and 100 mM suspended sulphur at 3000 rpm. Scans were performed at 10 mV s^{-1} in a range of −1.5 to 1.0 or 1.2 V. Red arrows show scan direction. Potential is vs Ag/AgCl, 3 M NaCl.

$E_{P.CS}$ appeared centred at −1.0 V. Note that the appearance of a peak instead of a plateau during rotation strongly indicates that the species being reduced are (ad)sorbed to the electrode surface [32]. This strengthens the hypothesis that the cathodic peak is the result of reduction of sulphur being deposited on the electrode surface during oxidation of sulphide. The selectivity of oxidation of sulphide to electrochemically active sulphur could be derived from the ratio between the cathodic and anodic peak area at a rotating electrode (Eq. (5) and (Eq. (6). From the CV of 0.3 mM sulphide at 3000 rpm it was calculated that the product selectivity of sulphide oxidation towards sulphur was at least 25 ± 7 %.

DCV of sulphide

By performing the first derivative of the CV, potentials were determined from the inflection points, so the highest change in reaction rate. These were made visible to amplify and better visualize the sensitivity of voltage change on current signal. The DCV of 0.3 mM sulphide at 3000 rpm and 10 mV s^{-1} (Fig. 2D-E) showed a slight anodic peak $E_{i.AS}$ at 0.35 V, and a broad cathodic peak $E_{i.CS}$ centred at −0.75 V, meaning that at these potentials the oxidation and respectively reduction started.

3.1.3. *(Poly)sulphide*

CV was performed on a mixture of sulphide and polysulphides at chemical equilibrium, denoted as (poly)sulphide. The voltammograms of the (poly)sulphide mixture at 0 rpm (Fig. 3A) showed two anodic peaks: $E_{P.AP1}$ starting at −0.3 V and centred at −0.10 V with peak current of 6 µA, and a broad peak $E_{P.AP2}$ at 0.24 V with peak current of 10 µA. Additionally, the voltammogram showed one intense cathodic peak $E_{P.CP}$ at −0.92 V with a peak current of −27 µA. At a pH of 8.5 and a pK_x of 8.82 [33] about 32 % of (poly)sulphide is in the form of polysulphide and 68 % is sulphide. Both species can oxidise to sulphur, thiosulphate, sulphite and sulphate. No sulphite and thiosulphate peaks were observed, so either sulphur or sulphate was formed during oxidation. As sulphate is electrochemically inert, the cathodic peak $E_{P.CP}$ can be assigned to reduction of sulphur to sulphide. Polysulphides can also be reduced to polysulphides with a shorter chain length [34] (Table 1, R4), which would be visible as a cathodic peak in the forwards scan during CV. However, no cathodic current other than background signal was observed in the forward scan of the first cycle, which implies that polysulphides were not electrochemically reduced at a GC electrode.

Based on thermodynamic calculations (SI section S.1) the equilibrium potential E_{eq} of sulphide-sulphur redox couple is −0.45 V, whereas for the polysulphide-sulphur redox couple the E_{eq} is −0.47 V, and further oxidation of sulphur to sulphate is possible at potentials higher than −0.59 V. Therefore, both $E_{P.AP1}$ and $E_{P.AP2}$ could be related to the oxidation of sulphide and polysulphide. Peak $E_{P.AP2}$ at 0.24 V was similar to peak $E_{P.AS}$ centred at 0.26 V, which was attributed to oxidation of sulphide to both sulphur and sulphate. As peak $E_{P.AP1}$ was only observed in the presence of (poly)sulphide, this peak is attributed to oxidation of polysulphide. To see if oxidation of polysulphide in peak $E_{P.AP1}$ led to sulphur formation, CV was performed in a smaller potential range of −1.5 to 0 V. Aside from anodic peak $E_{P.AP1}$ at −0.10 V at a current of 10 µA, one cathodic peak was observed of ~ 5 µA (corrected for background signal) at −0.87 V. This reduction peak is centred between $E_{P.CP}$ at −0.92 V and $E_{P.CS}$ at −0.84 V, both assigned to sulphur reduction to sulphide. Therefore, we speculate that $E_{P.AP1}$ is attributed to oxidation of polysulphide to sulphur and sulphate.

Different from the voltammogram of sulphide, in the voltammogram of (poly)sulphide solution 94 ± 5 % of anodic charge was recovered as cathodic charge at 0 rpm and 103 ± 31 % at 500–6000 rpm. This implied that the redox process was electrochemically reversible and the main product of (poly)sulphide oxidation was elemental sulphur or long chain polysulphides (Table 1, R4). This is interesting, as theoretically only 32 % of the (poly)sulphide present was polysulphide. For the other 68 %, sulphide, the ratio between anodic and cathodic current was only 39 ± 7 % (3.1.2). As sulphide oxidation yields one sulphur atom per two electrons and polysulphide on average about 5 sulphur atoms per two electrons [33,35,36], overall sulphur precipitation is 5 times faster per mol polysulphide than per mol sulphide. This could explain why the amount of sulphur reduced to sulphide in peak $E_{P.CS}$ was higher for (poly)sulphide than for sulphide.

Redox behaviour of (poly)sulphide at different rotation speeds

Similar to sulphide, the peak current of 1 mM (poly)sulphide increased when the rotation speed increased from 0 to 500 rpm and further increasing the rotation speed to 3000 did not increase the peak current. But different to sulphide oxidation, the anodic current of (poly) sulphide oxidation reached a plateau in the forward scan, followed by a decline to zero during the backward scan. This indicated that not electron transfer but another process hindered current production. When starting with the backward scan from + 1.0 to −1.5 V on a freshly polished electrode (Fig. S3), high currents were recorded directly from + 1.0 V. So it we postulate that the anodic current plateau for 500–3000 rpm and the anodic peaks at 4000–6000 rpm observed in Fig. 3B were caused by electrode passivation by a growth of an insulating sulphur layer. Of the anodic charge 103 ± 31 % was recovered in the cathodic charge peak, which indicated the formation of sulphur as product of (poly)sulphide oxidation. Sulphur is known to passivate electrodes upon precipitation [37], and indeed, the contribution of sulphur to the elemental composition of the electrode surface increased during CV (XRF, S.3). In section 3.1.4 the need for research on the characteristics and distribution of the sulphur layer is further discussed.

Interestingly, the voltammograms for (poly)sulphide at different rotation speeds (Fig. 3B) were similar for scans between 500 and 2000

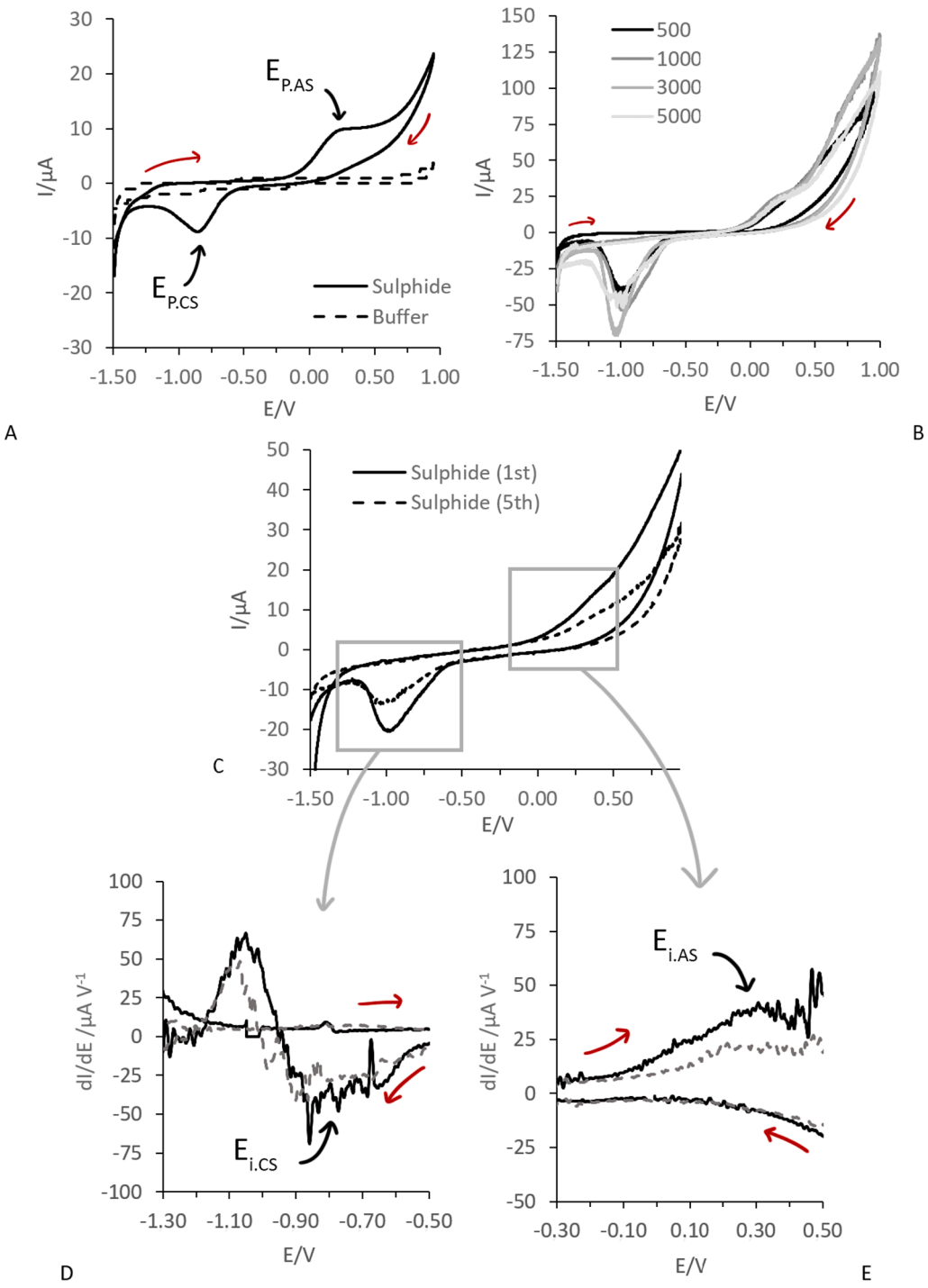

Fig. 2. Cyclic voltammograms of sulphide (S). A) 1 mM sulphide at 0 rpm. B) 1 mM sulphide at 500–5000 rpm. C) The first (line) and fifth (dashes) cycle of 0.3 mM sulphide at 3000 rpm. D) First derivative of cyclic voltammogram (DCV) of anodic current as shown in panel C. E) DCV of cathodic current as shown in panel C. All scans were performed in a range of −1.5 to 1.0 V at 10 mV s^{-1}. The red arrows show scan direction. Anodic (A) and cathodic (C) peak potentials E_P and inflection points E_i are indicated. Potential is vs Ag/AgCl, 3 M NaCl.

rpm, reaching a maximum anodic current of 23–33 µA at 0 V, showing a decline in current from 0.5 V onwards and reaching zero current at 0.5 V in the backward scan. But at CV scans at 4000 and 6000 rpm, a different anodic pattern was detected. Here, a clear peak of 70–72 µA (0.55–0.57 mA cm^{-1}) appeared at 0.25 V, and current declined to zero at 0.5 V during the forward scan. It seemed (poly)sulphide oxidation crossed a certain kinetic threshold between 2000 and 4000 rpm, causing oxidation to go faster and the sulphur layer to grow thicker more rapidly. Alternatively, the sulphur formation rate could have been limited by (reactive) intermediates that stick and/or accumulate at the electrode surface, but are no adherent to the electrode surface at higher rotation rates.

Whereas for the CVs with 1.0 mM sulphide at 500 rpm (Fig. 2B) on the voltammograms a symmetrical cathodic peak $E_{P.CS}$ appeared at −1.0 V, the scans of 1.0 mM (poly)sulphide at 500–6000 rpm showed a cathodic peak at potentials lower than −1.35 V. The peak was asymmetric and showed a shoulder at higher potentials up to −0.5 V. The presence of the shoulder was more pronounced when starting a fresh run

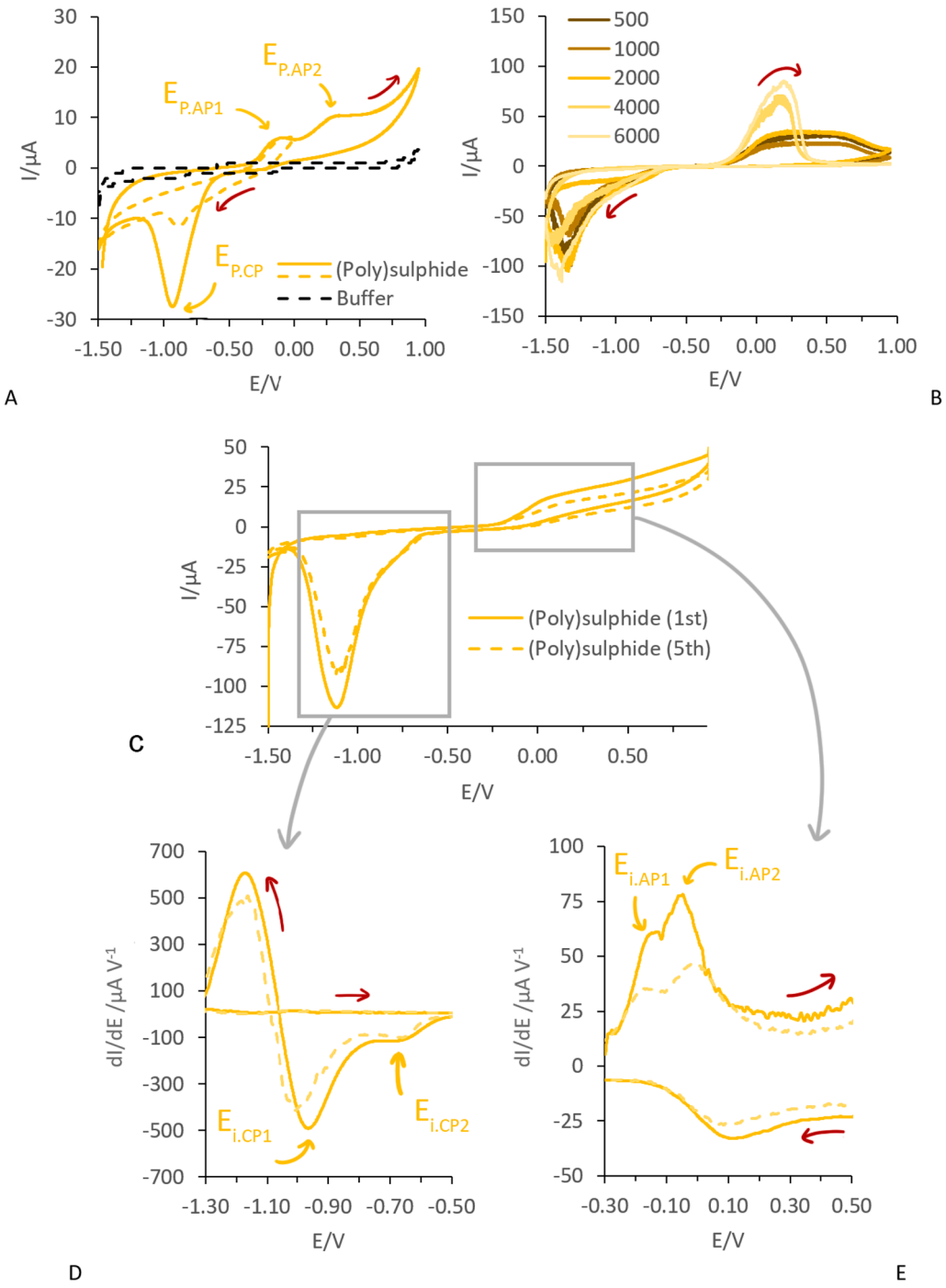

Fig. 3. Cyclic voltammograms of (poly)sulphide (P). A) 1 mM (poly)sulphide at 0 rpm. B) 1 mM (poly)sulphide at 500–6000 rpm. C) The first (line) and fifth (dashes) cycle of 0.3 mM (poly)sulphide at 3000 rpm. D) DCV of anodic current as shown in panel C. E) DCV of cathodic current as shown in panel C. All scans were performed in a range of −1.5 to 0.0 or 1.0 V at 10 mV s^{-1}. The red arrows show the scan direction. Anodic (A) and cathodic (C) peak potentials E_P and inflection points E_i are indicated. Potential is vs Ag/AgCl, 3 M NaCl.

with the backward scan, where instead of shoulders clear peaks are seen (Fig. S3). We postulate that different sulphur allotropes with different electrochemical properties were formed in the presence of sulphide and (poly)sulphides.

DCV of (poly)sulphide

The voltammogram of 0.3 mM (poly)sulphide (Fig. 3C), obtained at 10 mV s^{-1} and 3000 rpm, reached an oxidative current plateau from 0.07 V onwards. Contrary to scans of 1.0 mM (poly)sulphide, here the current did not go to zero before approaching $E_{P.AP1}$ around −0.1 V and therefore it can be argued that at 0.3 mM and 3000 rpm (poly)sulphide oxidation was limited by diffusion, however this needs to be confirmed by further studies at different rotation speeds. In the DCV obtained at 0.3 mM and 3000 rpm (Fig. 3D-E), two peaks were observed during the forward scan: $E_{i.AP1}$ of −0.13 V and $E_{i.AP2}$ of 0.03 V. We speculate that the oxidation of (poly)sulphide involved multiple steps and (reactive) intermediates, leading to two inflection points in the voltammogram. Also, in the first derivative of the cathodic current two distinct peaks $E_{i.CP1} = -1.0V$ and $E_{i.CP2} = -0.65V$ appeared, which implied the reduction of different sulphur allotropes.

3.1.4. Outlook on characterisation of sulphur redox processes

Sulphur electrochemistry is complex with its reaction mechanisms being dependent on, among others, supporting electrolyte composition and electrode material [38]. Research on sulphur redox couples is ubiquitous [38–40], yet there is still no full consensus on the reaction mechanisms of the electrochemical oxidation or reduction of sulphur species, especially at bioelectrochemically relevant conditions (ambient temperature and pressure, aqueous solutions). Most of the research has been conducted in high dielectric solvents such as organic solvents or ionic liquids due to sulphur being poorly soluble in aqueous solutions. Consequently, there is little experimental evidence on (bio)electrochemical reaction mechanisms of sulphur redox couples in aqueous and especially haloalkaline media, even less using glassy carbon electrodes.

In this work, we investigated the redox behaviour of sulphide and (poly)sulphide in haloalkaline media to be able to interpret the redox behaviour of sulphide shuttling SOB. For this purpose, it was sufficient to gain a 'fingerprint' of sulphide and (poly)sulphide in the form of DCV, and compare it to the fingerprint of sulphide shuttling SOB. Nevertheless, the insights from this work form a basis for further investigating sulphur redox behaviour in haloalkaline solutions. Further characterisation of the redox mechanisms of (poly)sulphide would need an extensive and systematic cyclic voltammetry study, i.e. at different scan rates, rotation speeds, pH, and reactant concentrations. Mechanistic information could then be extracted from change in peak potential, current, width, and area [41].

Furthermore, *in situ* measurements could give more insight into intermediates and products formed. From the data shown in this work it was not possible to determine which specific sulphur/polysulphide reduction reaction is associated with which cathodic peak. However, we can conclude that the sulphur layers produced in the presence of only sulphide and (poly)sulphides had different characteristics [42]. The differences in sulphur layer characteristics could be caused by formation of different sulphur allotropes due to (local) variations in, among others, pH, ionic strength, potentials, reaction rate, and electrode composition. For example, Buckley et al. (1987) observed that the sulphur layer formed on top of a gold electrode surface consisted of different zones with different characteristics. The initial layers of sulphur behaved like gold-sulphide, and on top of that layer a sulphur layer grew with different characteristics from bulk elemental sulphur. It was proposed that the initial metal-sulphide layer has catalytic properties for sulphur formation [43]. Similarly, carbon–sulphur layers are formed on the surface of glassy carbon electrodes [44]. Therefore, it could be extrapolated that the initial sulphur layer on the GC electrode served as a catalytic layer for further sulphur deposition. For further investigation of sulphur redox behaviour, Raman spectroscopy or confocal Raman microscopy could be used to measure sulphur allotropes and intermediates formed during (poly)sulphide oxidation in-situ [45,46]. Additionally, the distribution of the chain length of polysulphides could be determined with a HPLC based method [47].

3.2. Electrochemistry of sulphide shuttling SOB at glassy carbon

As shown above, DCV of sulphide and of (poly)sulphide produced two different 'fingerprints'. Where sulphide only had one anodic peak ($E_{i.AS} = 0.35V$) and one broad cathodic peak ($E_{i.CS} = 0.75V$), in the first derivative of the CV, (poly)sulphide showed two anodic peaks ($E_{i.AP1} = -0.13V$ and $E_{i.AP2} = 0.03V$) and two cathodic peaks ($E_{i.CP1} = -1.0V$ and $E_{i.CP2} = -0.65V$) therein. These 'fingerprints' of sulphide and (poly)sulphide are therefore adequately different to be used to detect the presence of sulphide and polysulphide separately. In the following section, the mechanisms underlying sulphide shuttling by SOB are further elucidated by comparing voltammograms and DCVs of sulphide, (poly) sulphide, and sulphide shuttling SOB.

3.2.1. SOB catalyse polysulphide formation

Before biotic CVs, i.e. CVs in solutions containing SOB, were performed, SOB were incubated with 0.2–0.3 mM sulphide to create sulphidic conditions. In 15 min 0.15–0.2 mM sulphide was removed from solution, and 0.02–0.15 mM sulphide was still in solution at the start of CV, as measured by colorimetric assay. At a first glance, the voltammograms of sulphide and sulphidic SOB did not differ remarkably (Fig. 4A). In the first cycle, the anodic current increased with potential starting at about 0 V and a cathodic peak of the presumably adsorbed oxidation products appeared, similar to $E_{P.CS}$ observed for sulphide. It is very plausible that the sulphide peak was at least partly caused by oxidation of sulphide left in solution. However, in the first derivative of the CV (Fig. 4C-D), the sulphide oxidation peak $E_{i.AS}$ centred at 0.35 V did not appear in the presence of SOB. Instead, in seven of the nine sulphidic SOB samples, a small anodic peak $E_{i.AX} = -0.1V$ appeared, similar to $E_{i.AP1}$ of (poly)sulphide. Additionally, two peaks appeared in the DCV of backward scan (Fig. 4F) at $E_{i.CX1} \approx -0.7V$ and $E_{i.CX3} \approx -1.0V$, again similar to $E_{i.CP1}$ and $E_{i.CP2}$ found for (poly)sulphide. With increasing number of cycles , the sulphide-like signal decreased and the (poly)sulphide-like signal started to dominate (Fig. 4D and F). The total current output decreased as well. The decrease in anodic current could have been caused by loss of sulphide as it was flushed out of the headspace. But, as deduced from the voltammograms obtained in the presence of sulphide, sulphide is converted to both sulphur and sulphate, the latter is an electrochemically irreversible process and causes the bulk sulphide concentration to decrease. It was observed for sulphidic SOB that after four to ten consecutive cycles the oxidative current disappeared and only the background signal remained (Fig. 4B). From that point on, the voltammograms slowly formed a cathodic current plateau at < -0.5 V (Fig. 4B), similar to aerated bicarbonate buffer (Fig. S8). This was likely the result of the influx of oxygen.

SOB likely contain elemental sulphur, even after thorough aeration [11]. The presence of S^0 in samples containing SOB could have facilitated the formation of polysulphides during sulphide removal. The chemical equilibrium reaction between sulphide and (bio)sulphur to form polysulphide (Eq. (1)) is relatively fast and can be complete in 20–30 min [48]. SOB were incubated with sulphide for 15 min prior to CV, which means there was enough time for polysulphides to be formed by chemical equilibration. To test the involvement of sulphur stored in SOB in the formation of polysulphides, a control was performed where instead of SOB biologically produced sulphur (biosulphur) was added. When adding biosulphur instead of SOB, no polysulphide signal was detected after incubation (Fig. S7). This showed that polysulphide formation was caused by microbial activity and chemical equilibration was not sufficient to explain the observed polysulphide signal. Furthermore, when no rotation was applied the voltammogram of sulphidic SOB did not show a polysulphide peak, also not in later cycles (Fig. 5A). This could indicate that the concentration of polysulphides was too low to be detected, or that the polysulphides were not free to diffuse through the solution. Biotic samples did show a polysulphide signal when rotation was applied and cells were brought into contact with the electrode surface by convection, therefore it can be postulated that the polysulphides detected in biotic samples were attached to or stored in the bacteria. Recently it was discovered that the distribution of polysulphide chain-length is influenced by SOB [47], which supports the hypothesis that SOB interact with certain polysulphides. From the data obtained in this work it is not possible to determine which polysulphides were formed or sorbed to the biomass. In future research, the speciation of adsorbed (poly)sulphide species could be investigated using HPLC based methods to detect sorbed sulphur species [49] and determine polysulphide speciation [47].

Based on the total charge of the anodic and cathodic current measured during CV (Eq. (8)) the selectivity of the oxidation of sulphide to sulphur by sulphidic SOB varied between 18 and 77 % (averaged 42 ± 20 %), and was therefore in most cases higher than the sulphur selectivity from sulphide in the absence of SOB (25 ± 7 %). This implies that SOB catalyse sulphur formation on the electrode surface. Previously it was proposed that the sulphide shuttling capabilities of SOB could be

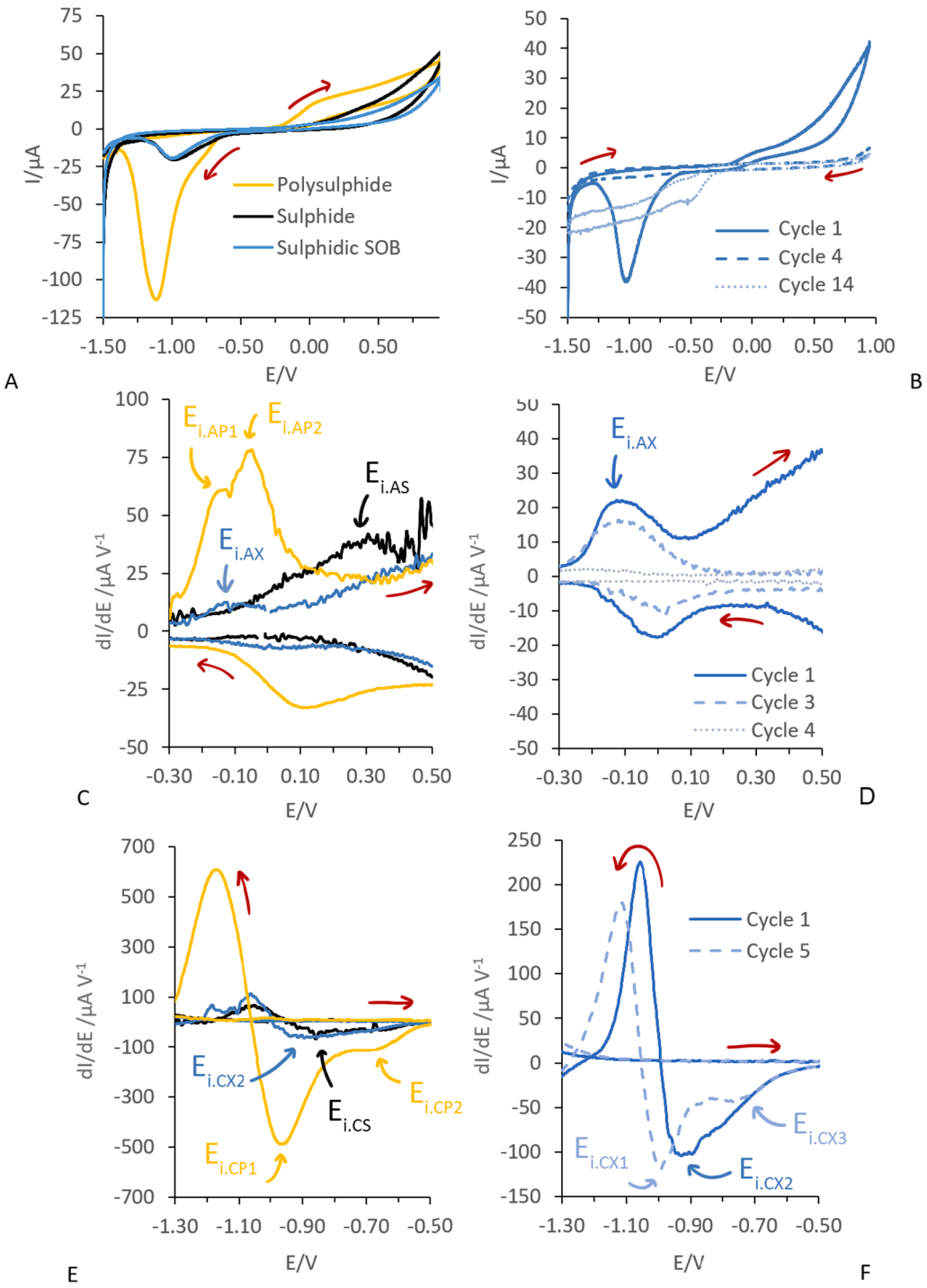

Fig. 4. A) Cyclic voltammogram of 0.3 mM sulphide (S), 0.3 mM (poly)sulphide (P), and sulphidic SOB (X) incubated with 0.2–0.3 mM sulphide at 10 mV s^{-1} and 3000 rpm. B) A representative example of a cyclic voltammogram of 60 mgN L^{-1} SOB incubated with 0.3 mM sulphide. C) DCV of anodic region of panel A. D) DCV of anodic region of a representative biotic sample. E) DCV of cathodic region of panel A. F) DCV of cathodic region of a representative biotic sample. More biotic samples are shown in Fig. S5 and S6. Anodic (A) and cathodic (C) inflection points E_i are indicated. In B, D, and F multiple cycles of the same run are shown, as noted in the legenda. All scans were performed from −1.5 to 1.0 V and back, as shown by the red arrows, at a scan rate 10 mV s^{-1} and 3000 rpm. Potential is vs Ag/AgCl, 3 M NaCl.

exploited in the development of a bioelectrochemical desulphurisation system [26]. It was proposed that by spatially separating sulphide removal and electron transfer, current could be harvested in the absence of sulphide, which could prevent electrode passivation by sulphur precipitation. However, based on our results, biological sulphide shuttling may still result in sulphur deposition and other strategies to prevent sulphur deposition need to be developed.

3.2.2. *Aerated SOB can be electrochemically reduced*

Interestingly, aside from the peaks $E_{i.CB}$ around −0.7 V associated with the presence of small amounts of oxygen in the solution (Fig. S8), the first derivatives of CVs of aerated SOB showed a peak $E_{i.CX4}$ around −0.4 V (Fig. 5C) indicating that aerated SOB could be electrochemically reduced. This peak did not occur for the same SOB in sulphidic state. Only in one case did we observe the appearance of $E_{i.CX4}$ during the scan

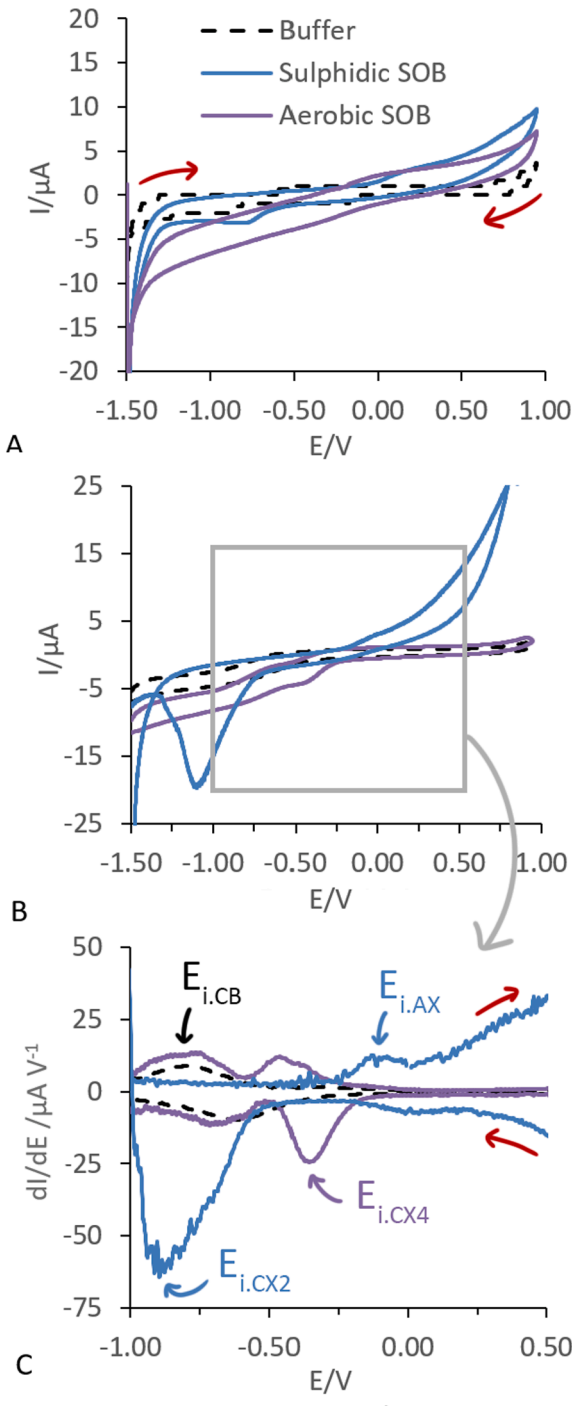

Fig. 5. A) Cyclic voltammograms of buffer (B) and 40–60 mgN L^{-1} aerated or sulphidic SOB (X) at 0 rpm. B) Cyclic voltammograms of buffer, sulphidic SOB, and aerated SOB (see also Fig. S9) at 3000 rpm. C) DCV of cyclic voltammograms shown in B. Scans were performed from −1.5 to 1.0 V and back at a scan rate 10 mV s^{-1}. The red arrows indicate the scan direction. Indicated the anodic (A) and cathodic (C) infection points E_i. Potential is vs Ag/AgCl, 3 M NaCl.

of sulphidic SOB, and this was 10 consecutive cycles after the sulphur species-like signal disappeared and a cathodic current plateau appeared at < −0.5 V, indicating the presence of oxygen (Fig. 4B). Which reduction reactions were happening at peak $E_{i.CX4}$ is not known, but these reactions only happened for aerated SOB, which indicates that either oxygen was needed in one of the reactions for the reduction process to occur, or that the exposure to sulphide inhibited the ability of SOB to be reduced.

It is postulated that aside from storage of polysulphides, sulphide shuttling SOB store electrons in electron carriers such as cytochromes and quinones. Further research is needed to elucidate the link between uptake of electrons and release of electrons to an electrode by SOB. Raman spectroscopy can be used to determine the reduction level of cytochromes [50]. Measuring the cytochrome reduction level of SOB with Raman spectroscopy before and after electrochemical reduction could give a more conclusive answer on the role of cytochromes in electron uptake by SOB.

3.3. Conclusions

The redox behaviour of sulphide shuttling SOB was investigated by performing cyclic voltammetry at a glassy carbon rotating disc electrode at haloalkaline conditions and the results were compared to abiotic sulphide and (poly)sulphide redox behaviour. As summarised in Scheme 2, in this work the RDE was used to distinguish between redox behaviour of sulphide and (poly)sulphide, to facilitate direct contact between SOB and electrode surface, and to detect the presence of sulphur adsorbed to the electrode surface.

At the conditions tested in this study, sulphide oxidation was possible for potentials more positive than −0.1 V and was electron transfer limited (1), whereas polysulphide oxidation already occurred from −0.3 V onwards and was possibly limited by diffusion at low concentrations (2). The differences between voltammogram shape (peak potentials and inflection points) of sulphide and (poly)sulphide made it possible to detect the presence of sulphide and polysulphide independently. The DCV of sulphidic SOB was dominated by sulphide-like response during the first cycles. Additionally, a small polysulphide-like signal was present, which became more dominant as cycles progressed and the sulphide-like signal diminished.

Convection applied by rotation of the electrode facilitated direct contact between SOB and the electrode surface (3). It was observed that aerated, i.e. oxidised, SOB could interact with the electrode surface when rotation was applied and take up electrons at potentials lower than −0.4 V. This was not observed for sulphidic, i.e. reduced, SOB. Therefore, we postulate that the abilities to take up or transfer charge are linked to the oxidation state of SOB, the presence of oxygen, or the presence of sulphide. Additionally, the forced convection applied by rotation of the disc was used to indicate the location of polysulphides formed by sulphidic SOB. The polysulphide signal was only observed for sulphidic SOB when rotation was applied, which indicated that the polysulphides were not free to diffuse through the solution, and were attached to the biomass.

A cathodic peak was observed for voltammograms of (poly)sulphide, even at high rotation speeds of 5000 rpm, which indicated the

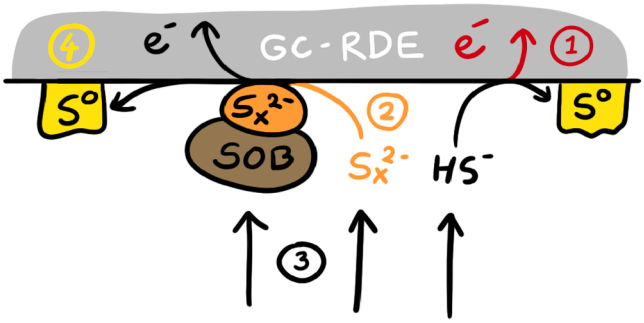

Scheme 2. Schematic representation of the use of the glassy carbon rotating disc electrode (in elucidating the electroactivity of sulphide oxidising bacteria (SOB). The convection applied by rotating the disc (3) brings solutes and suspended cells into contact with the electrode. The resulting current profile could be used to distinguish between sulphide oxidation (1) and polysulphide oxidation (2), as well showing the precipitation of sulphur upon the electrode surface (4).

precipitation or sorption of sulphur at the electrode surface (4). In the presence of sulphidic SOB, where part of the sulphide had been removed from solution, this peak also appeared. Therefore, we postulate that at least part of the sulphide removed by SOB was oxidised and precipitated as sulphur at the electrode surface.

We demonstrate that SOB catalysed the formation of polysulphide, that the polysulphides detected were adherend to the biomass, and that the polysulphides could be electrochemically oxidised at the electrode surface.

CRediT authorship contribution statement

Rikke Linssen: Writing – original draft, Visualization, Investigation, Formal analysis. **Sanne de Smit:** Supervision, Conceptualization. **Katharina Röhring (neé Neubert):** Methodology, Investigation, Formal analysis. **Falk Harnisch:** Writing – review & editing, Supervision, Methodology, Formal analysis. **Annemiek ter Heijne:** Writing – review & editing, Supervision, Funding acquisition.

Declaration of competing interest

The authors declare that they have no known competing financial interests or personal relationships that could have appeared to influence the work reported in this paper.

Data availability

The data will be uploaded to the 4TU.ResearchData depository after publication of the manuscript

Acknowledgement

This work is part of the research program Vidi (with project number 17516), which is (partly) financed by the Dutch Research Council (NWO). We would like to thank WIMEK for funding a research stay of Katherina Röhring at WUR (WIMEK research fellowship, category C). This work was supported by the Helmholtz-Association in the frame of the Integration Platform 'Tapping nature's potential for sustainable production and a healthy environment' at the UFZ. We especially acknowledge Reviewer #1, whose numerous thoughtful comments and great ideas have helped tilting this work to a higher level.

Appendix A. Supplementary data

Supplementary data to this article can be found online at https://doi.org/10.1016/j.bioelechem.2024.108710.

References

[1] D.Y. Sorokin, J.G. Kuenen, G. Muyzer, The microbial sulfur cycle at extremely haloalkaline conditions of soda lakes, Front. Microbiol. vol. 2, no. MAR (2011), https://doi.org/10.3389/fmicb.2011.00044.
[2] D.Y. Sorokin, J.G. Kuenen, Haloalkaliphilic sulfur-oxidizing bacteria in soda lakes, FEMS Microbiol. Rev. 29 (4) (Sep. 2005) 685–702, https://doi.org/10.1016/j.femsre.2004.10.005.
[3] D.Y. Sorokin, T.N. Zhilina, A.M. Lysenko, T.P. Tourova, E.M. Spiridonova, Metabolic versatility of haloalkaliphilic bacteria from soda lakes belonging to the Alkalispirillum-Alkalilimnicola group, Extremophiles 10 (3) (Jun. 2006) 213–220, https://doi.org/10.1007/s00792-005-0487-7.
[4] R. Rawat, S. Rawat, Colorless sulfur oxidizing bacteria from diverse habitats, Adv. Appl. Sci. Res. 6 (4) (2015) 230–235.
[5] C. Cline, A. Hoksberg, R. Abry, and A. Janssen, "Biological Process for H2S Removal from gas streams, The Shell-Paques/Thiopaq gas desulfurization process," in *Laurance Reid Gas Conditioning Conference*, 2003.
[6] R. De Rink, et al., Effect of process conditions on the performance of a dual-reactor biodesulfurization process, J. Environ. Chem. Eng. 9 (6) (2021) 106450, https://doi.org/10.1016/j.jece.2021.106450.
[7] R. De Rink, J.B.M. Klok, G.J. Van Heeringen, K.J. Keesman, Biologically enhanced hydrogen sulfide absorption from sour gas under haloalkaline conditions, J. Hazard. Mater. 383 (118) (2020) 121104, https://doi.org/10.1016/j.jhazmat.2019.121104.
[8] R. De Rink, et al., Increasing the Selectivity for Sulfur Formation in Biological Gas Desulfurization, Environ. Sci. Tech. 53 (8) (2019) 4519–4527, https://doi.org/10.1021/acs.est.8b06749.
[9] A. Ter Heijne, R. De Rink, D. Liu, J.B.M. Klok, C.J.N. Buisman, Bacteria as an Electron Shuttle for Sulfide Oxidation, Environ. Sci. Technol. Lett. 5 (8) (2018) 495–499, https://doi.org/10.1021/acs.estlett.8b00319.
[10] R. Linssen, T. Slinkert, C.J.N. Buisman, J.B.M. Klok, A. Ter Heijne, Anaerobic sulphide removal by haloalkaline sulphide oxidising bacteria, Bioresour. Technol. 369 (118) (2023) pp, https://doi.org/10.1016/j.biortech.2022.128435.
[11] R. Linssen, A. ter Heijne, Electric discharge by sulphide shuttling bacteria, J. Chem. Technol. Biotechnol. (2023), https://doi.org/10.1002/jctb.7505.
[12] J. M. Shively, "Prokaryote Inclusions: Descriptions and Discoveries BT - Inclusions in Prokaryotes," J. M. Shively, Ed., Berlin, Heidelberg: Springer Berlin Heidelberg, 2006, pp. 3–20. doi: 10.1007/3-540-33774-1_1.
[13] Annemiek. Ter Heijne, M. A. Pereira, Joao. Pereira, and Tom. Sleutels, "Electron Storage in Electroactive Biofilms," *Trends Biotechnol*, vol. 39, no. 1, pp. 34–42, 2021, doi: 10.1016/j.tibtech.2020.06.006.
[14] J.T. Babauta, H. Beyenal, Mass transfer studies of Geobacter sulfurreducens biofilms on rotating disk electrodes, Biotechnol. Bioeng. 111 (2) (2014) 285–294, https://doi.org/10.1002/bit.25105.
[15] P.S. Bonanni, D.F. Bradley, G.D. Schrott, J.P. Busalmen, Limitations for current production in Geobacter sulfurreducens biofilms, ChemSusChem 6 (4) (2013) 711–720, https://doi.org/10.1002/cssc.201200671.
[16] S. Boulêtreau, et al., Rotating disk electrodes to assess river biofilm thickness and elasticity, Water Res. 45 (3) (2011) 1347–1357, https://doi.org/10.1016/j.watres.2010.10.016.
[17] R.N.H. Daryono, A. Feurtet-Mazel, S. Bouletreau, F. Garabetian, Using an electrochemical assay to determine the biofilm elasticity change as a response to toxicant exposure, IOP Conf Ser Earth Environ. Sci. 156 (1) (2018) pp, https://doi.org/10.1088/1755-1315/156/1/012005.
[18] A.A.D. Jones, C.R. Buie, Continuous shear stress alters metabolism, mass-transport, and growth in electroactive biofilms independent of surface substrate transport, Sci. Rep. 9 (1) (2019), https://doi.org/10.1038/s41598-019-39267-2.
[19] L. Shen, et al., Anodic concentration loss and impedance characteristics in rotating disk electrode microbial fuel cells, Bioprocess Biosyst. Eng. 39 (10) (2016) 1627–1634, https://doi.org/10.1007/s00449-016-1638-1.
[20] R. Ganguli, B.S. Dunn, Kinetics of Anode Reactions for a Yeast-Catalysed Microbial Fuel Cell, Fuel Cells 9 (1) (2009) 44–52, https://doi.org/10.1002/fuce.200800039.
[21] M. Kasuno, et al., Characterization of the photoinduced electron transfer reaction from the photosynthetic system in Rhodobacter sphaeroides to an exogenous electron acceptor, J. Electroanal. Chem. 636 (1–2) (2009) 101–106, https://doi.org/10.1016/j.jelechem.2009.09.017.
[22] A. Prévoteau, A. Geirnaert, J.B.A. Arends, S. Lannebère, T. Van De Wiele, K. Rabaey, Hydrodynamic chronoamperometry for probing kinetics of anaerobic microbial metabolism - Case study of Faecalibacterium prausnitzii, Sci. Rep. 5 (July) (2015) 1–13, https://doi.org/10.1038/srep11484.
[23] A. Ramanujam, B. Neyhouse, R. A. Keogh, M. Muthuvel, R. K. Carroll, and G. G. Botte, "Rapid electrochemical detection of Escherichia coli using nickel oxidation reaction on a rotating disk electrode," *Chemical Engineering Journal*, vol. 411, no. October 2020, p. 128453, 2021, doi: 10.1016/j.cej.2021.128453.
[24] R.J. Thorne, H. Hu, K. Schneider, P.J. Cameron, Trapping of redox-mediators at the surface of Chlorella vulgaris leads to error in measurements of cell reducing power, PCCP 16 (12) (2014) 5810–5816, https://doi.org/10.1039/c3cp54938k.
[25] B. Meyer, Solid allotropes of sulfur [Online]. Available: Chem. Rev. 64 (4) (1964) 429–451 https://pubs.acs.org/sharingguidelines.
[26] R. De Rink, et al., Continuous electron shuttling by sulfide oxidizing bacteria as a novel strategy to produce electric current, J. Hazard. Mater. vol. 424, no. PA (2022) 127358, https://doi.org/10.1016/j.jhazmat.2021.127358.
[27] N.S. Lawrence, R.P. Deo, J. Wang, Electrochemical determination of hydrogen sulfide at carbon nanotube modified electrodes, Anal. Chim. Acta 517 (1–2) (2004) 131–137, https://doi.org/10.1016/j.aca.2004.03.101.
[28] C. Stang, F. Harnisch, The Dilemma of Supporting Electrolytes for Electroorganic Synthesis: A Case Study on Kolbe Electrolysis, ChemSusChem 9 (1) (Jan. 2016) 50–60, https://doi.org/10.1002/cssc.201501407.
[29] J. Boulegue, Solubility of Elemental Sulfur in Water at 298 K, Phosphorus and Sulfur and the Related Elements 5 (1) (Sep. 1978) 127–128, https://doi.org/10.1080/03086647808069875.
[30] J. Feng, D.C. Johnson, Oxidation of Thiosulfate to Sulfate at Glassy Carbon Electrodes, J. Electrochem. Soc. 142 (8) (1995) 2618–2621.
[31] R. Ojani, J.B. Raoof, A. Alinezhad, Catalytic oxidation of sulfite by ferrocenemonocarboxylic acid at the glassy carbon electrode. Application to the catalytic determination of sulfite in real sample, Electroanalysis 14 (17) (2002) 1197–1202, https://doi.org/10.1002/1521-4109(200209)14:17<1197::AID-ELAN1197>3.0.CO;2-A.
[32] F. Scholz, U. Schröder, R. Gulaboski, Electrochemistry of Immobilized Particles and Droplets (2005), https://doi.org/10.1007/b137048.
[33] A. Teder, The equilibrium between elemental sulfur and aqueous polysulfide solutions, Acta Chem. Scand. 25 (1971) 1722–1728.
[34] J. Liu, M. Li, X. Zhang, Q. Zhang, J. Yan, Y. Wu, Dithiothreitol-assisted polysulfide reduction in the interlayer of lithium-sulfur batteries: A first-principles study, PCCP 21 (30) (2019) 16435–16443, https://doi.org/10.1039/c9cp01036j.
[35] W.E. Kleinjan, A. De Keizer, A.J.H. Janssen, Equilibrium of the reaction between dissolved sodium sulfide and biologically produced sulfur, Colloids Surf. B Biointerfaces 43 (3–4) (2005) 228–237, https://doi.org/10.1016/j.colsurfb.2005.05.004.

[36] W. Giggenbach, "Optical Spectra and Equilibrium Distribution of Polysulfide Ions in Aqueous Solution at 20°," 1972. [Online]. Available: https://pubs.acs.org/sharingguidelines.
[37] P.K. Dutta, K. Rabaey, Z. Yuan, J. Keller, Spontaneous electrochemical removal of aqueous sulfide, Water Res. 42 (20) (2008) 4965–4975, https://doi.org/10.1016/j.watres.2008.09.007.
[38] O.J. Moreno-Piza, M.F. Suarez-Herrera, Electrochemical study of the redox processes of elemental sulfur in organic solvents using poly (3,4-ethylene-dioxy-thiophene) modified glassy carbon electrodes as working electrodes and ionic liquids as electrolytes, Electrochim. Acta vol. 436, no. September (2022) 141442, https://doi.org/10.1016/j.electacta.2022.141442.
[39] Y.C. Lu, Q. He, H.A. Gasteiger, Probing the lithium-sulfur redox reactions: A rotating-ring disk electrode study, J. Phys. Chem. C 118 (11) (2014) 5733–5741, https://doi.org/10.1021/jp500382s.
[40] P. Schön, F. Hintz, U. Krewer, Electrochemical analysis of the reaction mechanism of sulfur reduction as a function of state of charge, Electrochim. Acta 295 (2019) 926–933, https://doi.org/10.1016/j.electacta.2018.08.153.
[41] N. Elgrishi, K.J. Rountree, B.D. McCarthy, E.S. Rountree, T.T. Eisenhart, J. L. Dempsey, A Practical Beginner's Guide to Cyclic Voltammetry, J. Chem. Educ. 95 (2) (Feb. 2018) 197–206, https://doi.org/10.1021/acs.jchemed.7b00361.
[42] R. Steudel and B. Eckert, "Solid Sulfur Allotropes - Elemental Sulfur and Sulfur-Rich Compounds I," R. Steudel, Ed., Berlin, Heidelberg: Springer Berlin Heidelberg, 2003, pp. 1–80. doi: 10.1007/b12110.
[43] R.J. Remick, E.H. Camara, Electrochemistry of the sulphide/polysulphide couple, Illinois (1983).
[44] C. Quijada, J.L. Vázquez, Electrochemical reactivity of aqueous SO2 on glassy carbon electrodes in acidic media, Electrochim. Acta 50 (27) (2005) 5449–5457, https://doi.org/10.1016/j.electacta.2005.03.027.
[45] C. Nims, B. Cron, M. Wetherington, J. Macalady, J. Cosmidis, Low frequency Raman Spectroscopy for micron-scale and in vivo characterization of elemental sulfur in microbial samples, Sci. Rep. 9 (1) (2019) 1–12, https://doi.org/10.1038/s41598-019-44353-6.
[46] J.D. Pasteris, J.J. Freeman, S.K. Goffredi, K.R. Buck, Raman spectroscopic and laser scanning confocal microscopic analysis of sulfur in living sulfur-precipitating marine bacteria, Chem. Geol. 180 (1–4) (2001) 3–18, https://doi.org/10.1016/S0009-2541(01)00302-3.
[47] K.A.K.Y. Johnston, et al., Polysulfide Concentration and Chain Length in the Biological Desulfurization Process: Effect of Biomass Concentration and the Sulfide Loading Rate, Environ. Sci. Tech. 57 (36) (Sep. 2023) 13530–13540, https://doi.org/10.1021/acs.est.3c03017.
[48] W.E. Kleinjan, A. De Keizer, A.J.H. Janssen, Kinetics of the reaction between dissolved sodium sulfide and biologically produced sulfur, Colloids Surf. B Biointerfaces 43 (3–4) (2005) 228–237, https://doi.org/10.1016/j.colsurfb.2005.05.004.
[49] J. Rodriguez, J. Hiras, and T. E. Hanson, "Sulfite oxidation in Chlorobaculum tepidum," *Front Microbiol*, vol. 2, no. MAY, 2011, doi: 10.3389/fmicb.2011.00112.
[50] N.A. Brazhe, et al., Probing cytochrome c in living mitochondria with surface-enhanced Raman spectroscopy, Sci. Rep. 5 (Sep. 2015), https://doi.org/10.1038/srep13793.

Rikke Linssen After Rikke graduated from MSc Biotechnology, specialised in Process design, at Wageningen University in 2020 she started her PhD in bioelectrochemistry at the department of Environmental Technology at Wageningen University. Here she studies the electrochemical interactions between sulphide oxidising bacteria and electrodes.

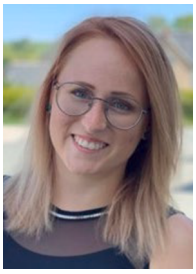

Sanne de Smit works as a Postdoc researcher at the Wageningen University. She got a Msc degree (2018) in Biotechnology with a thesis on microbial chain elongation and earned her PhD degree (2023) on the topic of Microbial Electrosynthesis from a self-obtained WIMEK grant. Her main research interests are bio-electrochemical solutions for treatment or reutilisation of various waste streams, e.g. CO_2, H_2S, NH_4^+. Within the field of bio-electrochemistry, she focusses on the combination of chemical and microbial catalysis within bio-electrochemical systems and the characterization of local conditions and gradients by e.g. microsensor measurements.

Katharina Röhring (neè Neubert) holds a B.Sc. (2015) and M. Sc. (2018), both in Biochemistry, from Leipzig University. Subsequently, she obtained her PhD in January 2023 also at Leipzig University under supervision of Falk Harnisch while working in the group 'Electrobiotechnology' at the Helmholtz Centre for Environmental Research – UFZ in Leipzig. During her PhD-studies she stayed 3 months with Annemiek ter Heijne at Wageningen University & Research (Netherlands). Her work focusses on application oriented research on electro-biorefineries, organic electrochemistry as well as electro-bioreactor design and engineering.

Falk Harnisch holds a Full Professorship at Leipzig University for Electrobiotechnology and is Co-Head of the Department of Microbial Biotechnology at the Helmholtz-Centre for Environmental Research – UFZ, Germany. He received his PhD from Greifswald University, Germany in 2009 as well as several fellowships and awards and was serving as a President of the International Society for Microbial Electrochemistry and Technology (ISMET). His research ranges from fundamentals of microbial electrochemistry via electroorganic synthesis to engineering of microbial electrochemical technologies.

Annemiek ter Heijne is professor at Environmental Technology, Wageningen University. Her research focuses on the recovery of valuable resources, like nutrients (nitrogen, sulfur) and energy, from wastewater, and to use electricity to convert CO_2 into useful chemicals and fuels. She is intrigued by the interaction between microorganisms and electrodes, allowing for new resource recovery technologies, and how the use of electrodes provides new ways to control and understand biological conversions.